

ANALYSIS OF LOCAL MECHANISMS THROUGH FLOOR SPECTRA FOR THE PRESERVATION OF HISTORICAL MASONRIES. A CASE STUDY

Mariateresa Guadagnuolo¹, Marianna Aurilio¹, Anna Tafuro¹ and Giuseppe Faella¹

¹ Department of Architecture and Industrial Design

University of Campania “Luigi Vanvitelli”

{mariateresa.guadagnuolo, marianna.aurilio, anna.tafuro, giuseppe.faella}@unicampania.it

Abstract

Non-structural masonry elements represent a significant part of the masonry cultural heritage due to their historical and artistic value. A significant portion of the total losses in recent earthquakes worldwide has been attributed to damage to non-structural elements, that are often very dangerous for public safety. These elements, i.e. merlons, pinnacles, sundial, gable, often undergo out-of-plane failures also for low values of peak ground acceleration. The assessment of the safety of these elements requires a correct evaluation of the seismic demand, to be performed considering the amplification and filtering effects due to the underneath structure, since they are often placed on the upper storeys of the buildings. To that end, the floor spectra are a powerful tool for assessing the earthquake acceleration and displacement requirements on non-structural elements. This paper focuses specifically on the linear and nonlinear kinematic analysis of freestanding masonry elements, comparing the previous Italian Building Technical Code (2008) with that of in force. The out-of-plane overturning mechanism of the protruding portion of the façade of a small chapel is studied, in order to better identify the main parameters that influence the evaluation of seismic safety of such a type of non-structural elements. The seismic demand in acceleration and displacement is computed by floor spectra both through a simplified approach and by using all modes assumed to be significant in the activation the out-of-plane mechanism of the considered protruding element.

Keywords: masonry building, freestanding elements, floor spectra, linear and nonlinear kinematic analysis.

1 INTRODUCTION

Recent earthquakes have shown the significant seismic vulnerability of historic buildings that characterize Italian urban centres. Based on seismic damage catalogued, this paper specifically investigates the damage mechanisms suffered by non-structural masonry elements in order to assess their effective vulnerability. According to NTC 2018 [1] “*non-structural elements are those with rigidity, strength and mass that significantly influence the structural response and those that, while not affecting the structural response, are equally significant for the safety and/or safety of people*”. Although this is a very relevant and common problem, literature papers and seismic codes are still in development. An in-depth analysis is then necessary to define reliable rules for modelling and analysing the most significant seismic effects on protruding elements such as merlons, pinnacles, sundial, gable, etc. Furthermore, the damage found is influenced by both the frequency component of each earthquake but also by the different characteristics of the building, which may vary depending on the period of construction, the materials and the morphology of the ground. The observed damage mechanisms are generally those due to the in-plane shear failure [2] and the out-of-plane overturning. Usually the most activated mechanism is the second one. The overturning mechanism of freestanding elements is more frequent and is dangerous for both the structural integrity of buildings (it has strong impact on the conservation) and for public safety, even because can occur with low values of peak ground accelerations.

In [3] there is an analysis of a group of castles, to find a relationship between construction features and damage and a table proposal is included to catalogue the main damage mechanisms identified in the castles affected by the 2012 earthquake in Emilia. However, this table was defined considering only a limited number of cases coming from the Emilia region; so it has a limited range of possible applications for cataloguing the damage caused by future earthquakes somewhere else and, above all, for the identification of all the vulnerable elements in order to undertake a preventive conservation [4, 5]. In [6, 7] the authors extended the study to two strong Italian earthquakes (Irpinia 1980 and Emilia 2012), considering a larger number of cases coming from different areas, implicitly considering different characteristics of the earthquake, ground type, distance from epicentre, type of construction, materials, technologies and state of conservation. In the paper [2], the number of seismic events considered has been further extended, including the earthquakes of Central Italy in 2016.

The protruding elements most studied in literature are the merlons and many studied examples are available: the castle of Arquata [8], the castle of Rancia in Tolentino (Figure 1) and the fortress of Visso [9].

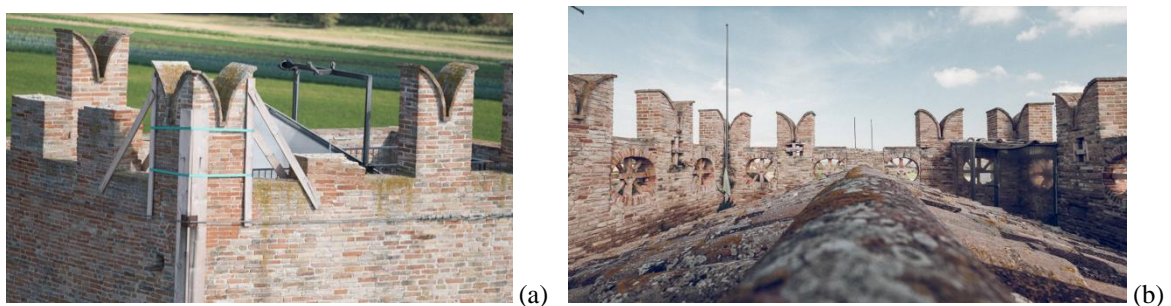


Figure 1: Rancia castle: (a) The merlons of the west tower; (b) The east façade with collapsed merlons [10].

Also in the case of the Castles of Giovannina (in San Giovanni in Persiceto), Pio (in Carpi), and Galeazza, the fortresses of Emilia and Reggiolo, the Gonzaga ducal palace (in Revere), referring to the earthquake of 2012, the Castle of Monte (in Montella), referring to the Irpinia earthquake of the 80's, in some masonry castles damaged by the Friuli earthquake and in the Castle of the Tower of Lorca, referring to the earthquake of Lorca in 2011, the seismic damage mechanisms are noticeable [2, 11].

Field surveys have shown that some seismic retrofitting interventions have not always been effective. In particular, the concrete ring beams introduced in the twentieth century were even harmful and, starting from the earthquake of Umbria-Marche in 1997 [12], seismic events have more highlighted how these interventions have been harmful. Unfortunately, several are the cases in which even strengthening interventions led to failure mechanisms or even the collapse of historic masonry buildings, as in the case of the San Felice sul Panaro fortress [13].

A paradigmatic example is the Urbisaglia Castle which has two different types of merlons: thin swallow-tailed merlons on the donjon and squat rectangular shaped merlons on the defensive walls (Figure 2). It is worth noting that only the thin ones were damaged by the earthquake. In theory, squat merlons should be more vulnerable to sliding shear failure. Nevertheless, no cases are reported in the analysed literature, even sliding shear damage could occur and, then, should be taken into account as possible failure mechanism for merlons. Considering all of this evidence, the case studies analysed in [2] show that damage and collapse of merlons can occur even with low values of peak ground accelerations (PGA), starting from about 0.05 g, especially for overturning mechanisms.



Figure 2: Urbisaglia Castle in Emilia [10]

From a structural point of view, blackbirds behave like a rigid block that can slide or rock and the oscillations of this type have been extensively studied in literature [14, 15]. Determining the type of dynamic response under earthquake is fundamental because it regulates the subsequent motion and the consequent type of failure. In the Ferretti et Al. paper [16] the rocking behaviour of blackbirds is studied performing nonlinear kinematic analysis.

Churches and palaces represent another important class of buildings that frequently suffered serious damage under earthquakes. Several times the existing heritage consists of

buildings with slender and non-structural elements at the top, as shown in Figure 3 and 4: these frequently have veils with bells or clocks, which mainly characterize relevant or municipal buildings. Furthermore, the study by Sorrentino et Al. [15] highlights that the damage in churches is often concentrated in the upper part of the façade. Finally, parapets are very vulnerable even in buildings that have been or reworked or strengthened, as can be seen even after the Canterbury earthquake [17].



Figure 3: (a) S. Giovanni in Laterano Palace, Rome; (b) Montecitorio Palace, Rome.



Figure 4: (a) City Hall, Rieti; (b) University of Bari, Bari.

Also Milani [18] has generally found that the façades (and in particular the tympanums) present an extremely high vulnerability. The reason is related both to the geometry of the façades and to the very poor or nonexistent connection with the perpendicular walls. Through three types of approaches, (linear kinematic analysis, global pushover analysis and FE upper bound limit analysis), it has been shown that, in almost all cases, the same failure mechanism is very likely. However, an important feature of all the analysis should be their ability to identify all those structural elements that can undergo a failure mechanism at low horizontal accelerations.

This paper investigates specifically the out-of-plane overturning mechanism of protruding portions of façades, in order to identify the main parameters that influence the assessment of their seismic safety. The focus is set on the linear and nonlinear kinematic analyses, comparing the previous Italian Building Technical Code [19] with that of in force [1].

2 KINEMATIC ANALYSIS OF FREESTANDING MASONRY ELEMENTS

The safety assessment of non-structural and secondary elements can be performed by the equilibrium limit analysis, according to the kinematic approach. This requires the choice of the collapse mechanism to be analysed, based on the possible presence of cracks, even of non-seismic nature, the quality of connection between walls, the presence of tie-rods and the interaction with other elements of the building or of adjacent buildings.

In this paper, the out-of-plane overturning mechanism of protruding portions of façades is analysed through linear and non-linear kinematic analysis, comparing the results obtained according to the 2008 and 2018 version of the Italian Building Technical Code [1, 19] and related Instructions [20, 21].

Linear kinematic analysis

The main changes between the two code versions mainly concern the seismic demand: the 2019 Instruction [20] explicitly takes into account the filtering effect exerted by the underneath structure, requiring to compute the floor response spectrum at the base of the examined element. The acceleration spectrum $S_{eZ}(T, \xi)$ at a given level z is computed by:

$$S_{eZ} = \sqrt{\sum S_{eZ,k}^2(T, \xi, z)} \quad (\geq S_e(T, \xi) \text{ for } T > T_1) \quad (1)$$

where:

$$S_{eZ,k}(T, \xi, Z) = \begin{cases} \frac{1.1 \xi_k^{-0.5} \eta(\xi) a_{Z,k}(Z)}{1 + [1.1 \xi_k^{-0.5} \eta(\xi) - 1] \left(1 - \frac{T}{aT_k}\right)^{1.6}} & T < aT_k \\ 1.1 \xi_k^{-0.5} \eta(\xi) a_{Z,k}(Z) & aT_k \leq T \leq bT_k \\ \frac{1.1 \xi_k^{-0.5} \eta(\xi) a_{Z,k}(Z)}{1 + [1.1 \xi_k^{-0.5} \eta(\xi) - 1] \left(\frac{T}{bT_k} - 1\right)^{1.2}} & T > bT_k \end{cases} \quad (2)$$

$$a_{Z,k}(z) = S_e(T_k, \xi_k) |\gamma_k \psi_k(z)| \sqrt{1 + 0.0004 \xi_k^2} \quad (3)$$

and $S_e(T, \xi)$ is the elastic response spectrum at the ground level, for the period T and the viscous damping ratio ξ of the element; T_1 is the first period of the structure; $S_{eZ,k}$ is the contribution to the floor response spectrum provided by the k^{th} vibration mode of the structure with T_k period and ξ_k damping; a and b are factors that define the range of maximum amplification of the floor spectrum, equal to 0.8 and 1.1 respectively; γ_k , $\psi_k(Z)$ and $\eta(\xi)$ are the k^{th} modal participation factor, the k^{th} modal shape and the damping correction factor of the main structure.

According to [20], the safety index, for each limit state (damage and mechanism activation), has to be evaluated as the ratio between the acceleration a_g , computed by Eqn (1), which equals the capacity of the mechanism in terms of acceleration and the peak ground acceleration (PGA).

The previous version [21] instead required that the following equation be satisfied:

$$a_0 = \frac{\alpha_0 g}{e^* F_C} \geq \frac{S_e(T_1) \psi(z) \gamma}{q} \quad (4)$$

where α_0 is the load multiplier that activates the mechanism, e^* is the fraction of participating

mass of the structure, FC is the confidence factor, $S_e(T_1)$ is the elastic response spectrum for the first period T_1 of the main structure, $\Psi(Z)$ is the first vibration mode of the main structure (advised to be assumed equal to $\Psi(Z) = Z/H$, where z is the height of the constraint lines between the block undergoing the mechanism and the remaining structure), γ is the modal participation factor of the main structure, equal to $3n/(2n+1)$, where n is the number of stories; q is the behavior factor, equal to 1 for the limit state of damage (LSD) and equal to 2 for the limit state of mechanism activation (LSA). Eqn. (4) immediately provides the safety index for both the limit states as ratio between capacity and demand in terms of acceleration.

Non-linear kinematic analysis

In the nonlinear kinematic approach, the behaviour of the protruding element is represented by a descending capacity curve in terms of seismic acceleration and displacement of a reference point, chosen as the mass center of the element. However, before the activation of the mechanism, the dynamic response of most protruding elements is substantially the one of a linear elastic cantilever; therefore, the 2019 Instruction requires the introduction of an initial linear elastic branch in the acceleration-displacement curve, linking the acceleration to the displacement by the period T_a of the freestanding element.

In both code instructions [20, 21], the capacity at LSA is evaluated on the acceleration-displacement curve, in correspondence of the lesser displacement between:

- the displacement $d_U = 0.40 d_0$, being d_0 the displacement at which the spectral acceleration is equal to zero [20, 21].
- the displacement corresponding to a reduction in capacity, in terms of acceleration, greater than 50% of the maximum value for the failure of some structural elements [20]; the displacement corresponding to locally incompatible situations for the stability of the element [21].

Moreover, the 2019 Instruction also requires the safety assessment at the limit state of collapse (LSC), assuming the displacement capacity equal to the lesser between $0.60 d_0$ and the one corresponding to locally incompatible situations for the stability.

In [20], the safety assessment is performed by computing the ground acceleration that produces a displacement demand on the mechanism equal to that corresponding to the achievement of the considered limit state (LSA or LSC). To this end, it is necessary to evaluate, on the capacity curve acceleration-demand, the characteristic equivalent period of the two limit states, suitably reduced with respect to those corresponding to the ultimate displacement, to consider the dispersion of results near the dynamic instability threshold:

$$T_S = k\pi \sqrt{\frac{d}{a(d)}} \quad (5)$$

where the factor k depends on the state limit, assuming 1.68 for the limit state of activation (LSA) and 1.56 for the limit state of collapse (LSC).

The demand is therefore computed by the acceleration spectrum at the level z (Eqn.1), transformed into a displacement spectrum, that is multiplying by $T^2/4\pi^2$:

$$d_E = S_{eZ}(T_S, \xi, z) \frac{T_S^2}{4\pi^2} \quad \left(\geq S_{eZ}(T_1, \xi, z) \frac{b^2 T_1^2}{4\pi^2} \text{ for } T_S > bT_1 \right) \quad (6)$$

As for the linear kinematic analysis, Eqn. (6) allows to evaluate the acceleration demand, for each limit state, and compare it to the peak ground acceleration (PGA).

In [21], instead, the displacement demand was to be computed on the displacement spectrum at the level z of the element, but the code allowed to perform the seismic assessment by means of the following equation:

$$d_U \geq S_{De}(T_1) \psi(z) \gamma \frac{(T_S/T_1)^2}{\sqrt{(1-T_S/T_1)^2 + 0.02 T_S/T_1}} \quad (7)$$

where the secant period $T_S = 2\pi(d_S/a_S)^{1/2}$ was computed for the displacement $d_S = 0.4 d_U$.

3 CASE STUDY

The updating proposed by the 2019 version of the Italian code for linear and nonlinear kinematic analysis is investigated by analysing a simple masonry building, that is a chapel in the outskirts of Nola, province of Naples. The church was built around the seventeenth century, as reported by the bell dated 1622, by the Count "Bracciolla". It was defined the "Second Porziuncola of St. Francesco" for its similarity and reduced dimensions compared to that of Assisi (Figure 5). It is a structure with single nave approximate 8 m long and consists of two rooms. The first, wider, devoted to liturgy, is 4.25 m wide, 5.00 m long and 4.00 m high. The second room, of a smaller size, is the sacristy and is 4.25 m wide, 1.75 m long and 3.45 m high. The walls are in tuff masonry, and are 0.45 m thick; the concrete roof is flat.



Figure 5: Chapel Second Porziuncola of St. Francesco in Nola: façade (a), detail of protruding element (b)

The façade has a total height of 6.05 m. The protruding element has a triangular shape similar to a tympanum, with a maximum height of 2.25 m, is 0.30 m thick and is leans on the roof at level of 3.80m.

Regarding the seismic input, the site has latitude 40.936503 and longitude 14.513228. Assuming the soil class A, the topographical category T1, Table 1 summarizes the seismic parameters computed for the three limit states considered in the following.

	$ag [g]$	F_0	$T_c^* [sec]$
LSD	0.067	2.318	0.312
LSA	0.180	2.382	0.355
LSC	0.227	2.452	0.363

Table 1: Values of seismic parameters

4 ANALYSIS AND RESULTS

The local mechanism involving simple overturning of the protruding part of façade of the studied chapel is envisaged in this section. Obviously, this mechanism do not cover the totality of the possible ones.

Initially, a dynamic characterization of the building was performed through a three-dimensional FE model. Figure 6 shows the first and third vibration mode: the first is translational in the transverse direction to the construction, the third, as the second one, is instead translational in the longitudinal direction. The fundamental period T_1 of the building is equal to 0.083 sec. The analysis allowed to select the modes assumed to be significant for the considered mechanism, i.e. those that activate the out-of-plane response of the considered protruding element. Table 2 contains the dynamic parameters of the modes used to compute the floor spectra (i.e. those that have the largest participation vector modes).

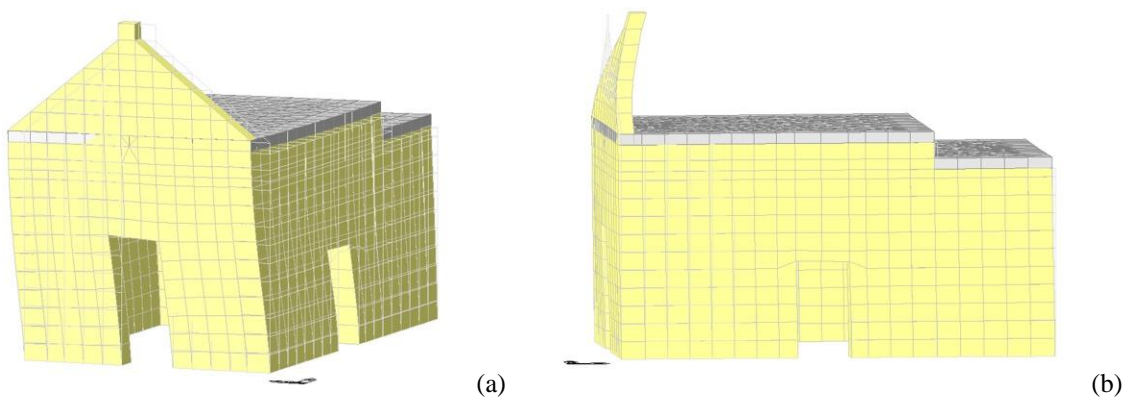


Figure 6: First and third vibration mode of the analysed chapel

Mode	T_K	γ_K	$\Psi_K(z)$	$\gamma_K \Psi_K(z)$
3	0.0613	-6.0443	-0.1750	1.0576
2	0.0757	6.5804	0.0207	0.1365
4	0.0530	-0.1665	-0.0907	0.0151
16	0.0257	-0.2138	-0.0185	0.0040
15	0.0260	-0.1624	-0.0058	0.0009
22	0.0216	-0.1251	-0.0049	0.0006

Table 2: Dynamic parameters of the modes assumed to be significant

From the structural point of view, the un-cracked freestanding portion can be modelled as a linear elastic cantilever while after cracking at the base it behaves as rigid blocks that could overturn with respect a cylindrical hinge at the top of facade.

The first period T_a of the protruding portion of façade estimated by means of the three-dimensional FE model (thus considering the actual triangular geometry of the element) is 0.070 sec, whereas the period determined by considering a cantilever of unit width and 1.75 m long is equal to 0.078 sec.

In the kinematic analyses, the block self-weight applied at its mass centre and the corresponding inertial horizontal force are only considered to act; dead and the live loads due

to the roof are assumed equal to zero because the masses associated to floor gravitational loads don't participate to the failure mechanism.

The presented results are based on the hypothesis of infinite compressive strength of masonry. Moreover, it is known that the out-of-plane response is influenced by the section morphology and the masonry quality, and the rotation axis could be back-warded with respect to the outside corner of the block. This would cause a reduction in the safety index, as well as a downward translation of the capacity curve.

The new code version [1, 20] requires to perform the safety assessment using the floor response spectra. The latter are strongly influenced by the non-linearity level of the main structure: they usually present a significant amplification in correspondence with the fundamental period of the elastic structure, which is reduced when the main structure enters the non-linear range of behaviour. The code takes into account this effect advising to assume elongated periods and incremented equivalent viscous damping of the main structure.

The increase in the fundamental period is nevertheless a crucial point: the increase is dependent on the level of shaking and the consequent extent of nonlinearity which is attained within the structure. However, this effect has been more frequently observed in experimental tests and theoretically studied for r/c buildings, while few data are available for masonry structures. Therefore, the modification of periods of the main structure could involve unreliable changes in the safety indexes. And in this context it must not be forgotten that the amplification on non-structural elements also depends on the relationship between the periods of the elements and the structure. Finally it should be considered that the elongation of the periods should be different for each limit state.

In the analyses that follow, in the absence of reliable data on this issue and wanting mainly to perform a comparison between the two versions of the Italian code, it was considered appropriate do not change the fundamental period of the building at LSD and to impose the same elongation of 50% (the minimum advised by [20]) at LSA and LSC.

On the other hand, it is important to take into account the effects of the nonlinear behaviour on the damping, considering the influence on both the floor spectrum (due to the non-linearity of the main structure) and the displacement demand (due to the non-linearity of the mechanism involving the protruding element). Few data are available for tuff masonry: therefore, comparing the two seismic codes, it was believed suitable to perform the analyses for a damping ξ_k of the main structure equal to 5% and 10%; the damping ξ_a of the mechanism has been constantly assumed equal to 5% in the linear kinematic analyses and equal to 8% and 10% (as required by the 2019 Instruction) in the nonlinear kinematic analyses respectively at LSA and LSC. This assumption is also based on the evidence that many protruding elements collapse for small values of acceleration, and therefore in almost total absence of damage to the main structure, especially as in the case under consideration, the construction being particularly low.

Linear kinematic analysis

Applying the principle of virtual work, the load multiplier α_o is equal to 0.20. Therefore, the acceleration a_o that activates the mechanism (Eqn. 4) is equal to 1.96 m/sec^2 (the fraction of participating mass of the structure e^* is equal to 1.0, the confidence factor FC has been assumed unitary).

According to [21], the safety indices I_s (capacity to demand ratio) at LSD and LSA, computed for $T_1 = 0.05 \text{ H}^{3/4} = 0.136 \text{ sec}$, $\Psi_k(z) = 1.00$ and $\gamma_k = 1$, are summarized in Table 3.

The 2019 code version requires to compute the seismic demand by means of floor response spectra (Eqn.1), considering all significant modes of vibration of the main structure. However,

for structures with masses uniformly distributed along the height (regular buildings), the code provides that a simplified approach can be used, neglecting the contribution of higher modes (because they are not very significant) and considering only the contribution of the first mode in the direction of interest. The code advises to assume the same expressions foreseen by [21] for the first vibration mode and the modal participation factor. However, the equation of the first vibration mode would be correct if it is not close to an inverted triangle.

Table 3 also contains the results of linear kinematic analyses performed according to [20]: I_S is the safety index computed considering all significant modes of vibration of the main structure (Table 2) while $I_{S,1}$ is computed using simplified values of $\Psi_k(z)$ and γ_k .

MIT 2009				MIT 2019						
	ξ_k	I_S	ξ_k	ξ_a	I_S	$I_{S,1}$	ξ_k	ξ_a	I_S	$I_{S,1}$
LSD	5 %	1.29	5 %	5 %	0.45	0.40			0.66	0.60
LSA		0.96			0.19	0.46	10 %	5 %	0.33	0.63

Table 3: Results of linear kinematic analyses

The difference in safety indices computed according to [20] and [21] is obviously due to the different method of calculating the demand: the new code version more correctly requires to compute it through floor spectra and not only referring to ground spectra, as considered in the past. Table 3 shows that the new I_S values are significantly smaller, regardless of the damping value ξ_k .

Table 3 also shows a not negligible difference between the safety indices at LSA computed, according to [21], considering all the significant modes (I_S) and those assessed according to the simplified approach ($I_{S,1}$). This is mainly due to the difference between the period of the most significant mode (0.061 sec) and the approximate value of the period used in the simplified approach (0.136 sec), also in relation to the period of the protruding element (0.078 sec). The above period, in fact, influences both the value of $Se(T_k, \xi_k)$ in Eqn (3) and the range of periods for which there is the largest amplification in the floor spectra. Its influence is also strongly dependent on the assumed elongation considering the non-linearity of the main structure.

Finally, a role in the difference between safety indices is also played by the parameters a and b which modify the range of maximum amplification of floor spectra (Eqn.2). The extension of the period range may or not involve the significant period of the structure and therefore may affect the amplification provided by the floor spectra. In the case under examination, the parameter a provides this type of influence.

The previous considerations highlight the importance of a reliable evaluation of the elongation of the most significant period of the main structure in the kinematic analysis of freestanding elements.

Nonlinear kinematic analysis

The displacement capacity of the mechanism is assessed, as required by both codes, on the acceleration-displacement curve ($d_U = 0.40 d_0$). According to [20], is equal to 0.06 m at LSA and 0.09 m at LSC, the secant periods T_S are respectively equal to 1.192 sec and 1.660 sec. While according to [21], d_U is equal to 0.06 m, $d_S = 0.40 d_U = 0.024$ m and the secant period T_S is equal to 0.897 sec.

Table 4 summarized the results provided by the nonlinear kinematic analysis in terms of safety indices I_S and shows that, in this case, the difference between the two codes at LSA is particularly small.

MIT 2009				MIT 2019							
	ξ_k	I_S	ξ_k	ξ_a	I_S	$I_{S,1}$	ξ_k	ξ_a	I_S	$I_{S,1}$	
LSA	5 %	1.50	5 %	8 %	1.39	1.39		10 %	8 %	1.39	1.39
LSC	-			10 %	1.23	1.23		10 %	10 %	1.23	1.23

Table 4: Results of nonlinear kinematic analyses

Moreover, referring to the procedure provide in [20], the results are the same both considering all the significant vibration modes and considering only the first one. In the present case, also the variation in the damping ξ_k of the main structure does not imply significant variations in the I_S indices. This is due to the particularly small magnitude of the displacement demand determined at the T_S periods, whereby changing the number of modes or the damping ξ_k the variation in displacement demand is at most irrelevant.

Linear kinematic analysis vs nonlinear kinematic analysis

In [20] it is stated that the simplified verification with behaviour factor through linear kinematic analysis should be performed when the capacity curve acceleration-displacement is not calculated, and only the multiplier that activates the mechanism is computed. And this simplification should be convenient for complex mechanisms, for which the execution of a nonlinear kinematic analysis would be problematic. The case study examined in this paper does not fall into this ambit: a nonlinear kinematic analysis should therefore preferably be carried out.

However, the above does not justify the marked difference in the values of the I_S indices computed through linear and non-linear kinematic analyses. Nor should the experience that indicates how frequently non-linear kinematic analyses lead to greater values of the capacity-to-demand ratio should be comforting. In the case under examination, in fact, the difference is very significant. This is due to the closeness of the fundamental period of vibration of the main structure (or that of the most significant mode) and the period of the protruding element. This closeness implies an amplification in the acceleration demand (linear kinematic) which does not correspond to an analogous amplification in terms of displacement demand (non-linear kinematic). Furthermore, the assessment of the displacement d_S at which to calculate the secant period T_S and the evaluation of the latter also seem to have a non-negligible role, since they can significantly affect the displacement demand.

5 CONCLUSIONS

The paper deals with the assessment of the seismic safety of freestanding masonry elements. For this purpose the protruding element of the façade of a small church is studied. The analyzes were carried out according to the linear and non-linear kinematic approach, also comparing the last Italian seismic code with the previous one.

A small and simple construction was deliberately analyzed to investigate in detail the main features of the new version of the code, that involves a significant improvement compared to the past, introducing more clearly the use of floor spectra in the evaluation of seismic demand. The simplicity of the construction also allowed clear indications to be given on some features of the verification procedure.

The analysis confirmed that the elongation of the vibration periods of the main structure, needed to consider the non-linearity of the structure's response, plays a particularly crucial role in the assessment of seismic safety. Especially for tuff masonry building for which few information is available on this topic.

As is known, in fact, the floor spectra provide the largest amplification in correspondence with the fundamental period of the main structure (or that of the most significant mode): therefore, in small and low buildings, such as the one examined here, generally characterized by the closeness between the period of the main structure and that of the protruding element, the assessment of the aforementioned elongation has an evident considerable influence.

For these constructions, moreover, the closeness between the two aforementioned periods implies an amplification in the acceleration demand which does not correspond to an analogous amplification in terms of displacement demand: this involves a significant difference among the safety indices computed by linear and nonlinear kinematic analyses. And this could lead to confusion in practical applications by professional technicians.

ACKNOWLEDGEMENTS

The contribute of Ministry of Education, University and Research and particularly the Basic Research Activities Fund (FFABR) is gratefully acknowledged.

REFERENCES

- [1] MIT, 2018. Norme Tecniche per le Costruzioni, DM 17.01.2018, Official Bulletin n. 42, 20.02.2018, (in Italian)
- [2] E. Coïsson, D.E Ferretti, E. Lenticchia, Analysis of damage mechanisms suffered by Italian fortified buildings hit by earthquakes in the last 40 years, 2017, Bull. Earthquake Eng., 15:5139–5166, 2017.
- [3] S. Cattari, S. Degli Abbatì, D. Ferretti, S. Lagomarsino, D. Ottonelli, A. Tralli, Damage assessment of fortresses after the 2012 Emilia earthquake (Italy). Bull. Earthquake Eng., 12(5):2333–65, <https://doi.org/10.1007/s10518-013-9520-x>, 2014.
- [4] G. Buonocore, A. Gesualdo, A. Iannuzzo, M. Monaco, M.T. Savino, Improvement of seismic performance of unreinforced masonry buildings using steel frames, Civil-Comp Proceedings, 106, 2014.
- [5] A. Gesualdo, M. Monaco, Seismic vulnerability reduction of existing masonry buildings. Modelling of retrofitting techniques COST ACTION C26: Urban Habitat Constructions under Catastrophic Events - Proceedings of the Final Conference, 853-858, 2010.
- [6] E. Coïsson, L. Ferrari, D. Ferretti, M. Rozzi, Non-smooth dynamic analysis of local seismic damage mechanisms of the San Felice fortress in Northern Italy. Proc. Eng. 161:451–457, doi:10.1016/j.proeng. 2016.08.589, 2016a.
- [7] E. Coïsson, D. Ferretti, E. Lenticchia, Italian castles and earthquakes: A GIS for knowledge and preservation. In: Van Balen K., Verstrynghe E. (eds) Structural analysis of historical construction SAHC 2016, 12–16 September 2016, Leuven. CRC Press/Balkema, Leiden, ISBN 978-113802951, 2016b.
- [8] A. M. D'Altri, G. Castellazzi, S. de Miranda, Collapse investigation of the Arquata del Tronto medieval fortress after 2016 central Italy seismic sequence, J. Build. Eng., 18:245–51, DOI:10.10106/j.jobe.2018.03.021, 2018.

- [9] E. Lenticchia, E. Coïsson, The use of GIS for the application of the phenomenological approach to the seismic risk analysis: the case of the Italian fortified architecture, *Int. Arch. Photogramm. Rem. Sens. Spatial Inf. Sci.*, XLII-5/W1:39-46, 2017.
- [10] M. Rota, Photographs of the Rancia Castle and the Torrione San Catervo in Tolentino. From: Lo stato delle cose. Geografie e storie del doposisma. Tolentino, il Castello della Rancia, 2017, www.lostatodellecose.com, Accessed Feb 2019.
- [11] X. Romão, A.A. Costa, E. Paupério, H. Rodrigues, R. Vicente, H. Varum, Field observations and interpretation of the structural performance of constructions after the 11 May 2011 Lorca earthquake. *Eng. Fail AnaL*, 34:670–92, 2013.
- [12] S. Tobriner, M. Comerio, M. Green, Reconnaissance report on the Umbria-Marche, Italy, Earthquakes of 1997. EERI Special Earthquake Report, 1997.
- [13] G. Castellazzi, A.M. D'Altri, S. de Miranda, F. Ubertini, An innovative numerical modeling strategy for the structural analysis of historical monumental buildings, *Eng. Struct.*, 132:229–48, <https://doi.org/10.1016/j.engstruct.2016.11.032>, 2017.
- [14] S. Lagomarsino, Seismic assessment of rocking masonry structures. *Bull. Earthquake Eng.*, 13(1):97–128, <https://doi.org/10.1007/s10518-014-9609-x>, 2015.
- [15] L. Sorrentino, D. D'Ayala, G. de Felice, M.C. Griffith, S. Lagomarsino, G. Magenes, Review of out-of-plane seismic assessment techniques applied to existing masonry buildings. *Int. J. Archit. Herit.*, 11(1):2–21, <https://doi.org/10.1080/15583058.2016.1237586>, 2017.
- [16] D. Ferretti, E. Coïsson, E. Lenticchia, Seismic damage on merlons in masonry fortified buildings: A parametric analysis for overturning mechanism, *Engineering Structures*, Elsevier, 15 December 2018.
- [17] D. Dizhur, N. Ismail, C. Knox, R. Lumantarna, J.M. Ingham, Performance of unreinforced and retrofitted masonry buildings during the 2010 Darfield earthquake. *B N Z Natl. Soc. Earthq. Eng.* 43:321–339, 2010.
- [18] G. Milani, M. Valente, Comparative pushover and limit analyses on seven masonry churches damaged by the 2012 Emilia-Romagna (Italy) seismic events: Possibilities of non-linear finite elements compared with pre-assigned failure mechanisms, *Engineering Failure Analysis* 47, 129–161, 2015.
- [19] MIT, 2008. Norme Tecniche per le Costruzioni, DM 14.01.2008, Official Bulletin n. 29, 04.02.2008, (in Italian)
- [20] MIT, 2019. Istruzioni per l'applicazione dell'aggiornamento delle Norme Tecniche per le Costruzioni di cui al D.M. 17.01.2018, C.S.LL.PP n. 7 21.01.2019, Official Bulletin n.35 11.02.2019, (in Italian).
- [21] MIT, 2009. Istruzioni per l'applicazione delle nuove Norme Tecniche per le Costruzioni di cui al D.M. 14.01.2008, C.S.LL.PP n. 617 02.02.2009, Official Bulletin n.47 26.02.2009, (in Italian).